



In-Vehicle Assessment of Human Exposure to EMFs from 25-kW WPT System Based on Near-Field Analysis

Preprint

Ahmed A. S. Mohamed and Andrew Meintz
National Renewable Energy Laboratory

Peter Schrafel and Anthony Calabro
Momentum Dynamics

*Presented at the 2018 IEEE Vehicle Power and Propulsion Conference (VPPC 2018)
Chicago, Illinois
August 27–30, 2018*

© 2018 IEEE. Personal use of this material is permitted. Permission from IEEE must be obtained for all other uses, in any current or future media, including reprinting/republishing this material for advertising or promotional purposes, creating new collective works, for resale or redistribution to servers or lists, or reuse of any copyrighted component of this work in other works.

**NREL is a national laboratory of the U.S. Department of Energy
Office of Energy Efficiency & Renewable Energy
Operated by the Alliance for Sustainable Energy, LLC**

This report is available at no cost from the National Renewable Energy Laboratory (NREL) at www.nrel.gov/publications.

Conference Paper
NREL/CP-5400-71710
August 2018

Contract No. DE-AC36-08GO28308

NOTICE

This work was authored in part by the National Renewable Energy Laboratory, operated by Alliance for Sustainable Energy, LLC, for the U.S. Department of Energy (DOE) under Contract No. DE-AC36-08GO28308. Funding provided by U.S. Department of Energy Office of Energy Efficiency and Renewable Energy Vehicle Technologies Office. The views expressed in the article do not necessarily represent the views of the DOE or the U.S. Government. The U.S. Government retains and the publisher, by accepting the article for publication, acknowledges that the U.S. Government retains a nonexclusive, paid-up, irrevocable, worldwide license to publish or reproduce the published form of this work, or allow others to do so, for U.S. Government purposes.

This report is available at no cost from the National Renewable Energy Laboratory (NREL) at www.nrel.gov/publications.

U.S. Department of Energy (DOE) reports produced after 1991 and a growing number of pre-1991 documents are available free via www.osti.gov.

Cover Photos by Dennis Schroeder: (left to right) NREL 26173, NREL 18302, NREL 19758, NREL 29642, NREL 19795.

NREL prints on paper that contains recycled content.

In-vehicle Assessment of Human Exposure to EMFs from 25-kW WPT System Based on Near-field Analysis

Ahmed A. S. Mohamed¹, Andrew Meintz¹, Peter Schrafel², Anthony Calabro²

¹ Transportation and Hydrogen Systems Center, National Renewable Energy Laboratory (NREL), Golden, CO, USA

² Momentum Dynamics, Malvern, PA, USA

Abstract—Wireless power transfer (WPT) technology has the potential to be a convenient and reliable charging method for the light and heavy duty electric vehicles. However, the loosely coupling between the two sides results in strong near-electromagnetic fields (EMFs) around the system, which may have the possibility to impact human safety if the standard limits are exceeded. Therefore, comprehensive tests are necessary to ensure the electromagnetic fields are within safe limits. Consequently, this paper presents a test methodology for the near-field from a 25 kW WPT system from Momentum Dynamics, which is installed in a heavy duty electric shuttle at the National Renewable Energy Laboratory (NREL). The paper describes in detail the measuring device, test setup and conditions. The misalignments between the two systems' sides are considered during the measurements. Test results for the regions of concern around and inside the bus are presented and compared with the reference levels defined by the international standards, including ICNIRP 2010 and IEEE C95.1. In addition, a finite-element model is developed for the wireless coupler and analyzed at the same conditions as the tests. Comparative analysis is presented between the simulated and experimental results. The measurements at the test points show adherence to the standard limits for the general public and occupational exposure.

Keywords—Electric Vehicles (EV); Electromagnetic Compatibility (EMC); Human Exposure; In-vehicle WPT; Wireless Power Transfer (WPT).

I. INTRODUCTION

Wireless power transfer (WPT) technology has the potential to be a convenient and reliable interface for electric vehicle (EV) charging. It provides several benefits over conductive charging: (1) the vehicle does not need to be parked in a certain location for a long time, (2) avoiding the manual plug provides safe operation in the presence of water, rain or dust, (3) it is reliable during storms, and (4) it is automatic and does not need the driver's intervention. Among the different WPT technologies, the inductive resonance technology is the most suitable for EVs applications since, it offers high power transfer capability through large air-gap (10-40 cm) situations, which is appropriate for EVs, and is maintenance free due to the absence of the mechanical parts [1], [2]. Inductive power transfer (IPT) is mainly based on the magnetic coupling between two isolated coils, which is characterized by a factor called coupling factor (k). Theoretically, this factor ranges from 0 to 1 based on the coil

design and the air-gap between them. In the conventional transformer, k is about 0.95 and it is called strongly coupled circuit, however, in IPT systems k ranges from 0.01 to 0.4 and it is termed as loosely coupled technology. The galvanic isolation in WPT systems provides safe, reliable, maintenance free operation in harsh environment. For these features, WPT technology is considered as an ideal solution for EV charging during the long-term parking (stationary), driving (dynamic) and transient stops (quasi-dynamic) [3]. Nevertheless, WPT for EV requires high electric power (up to few hundreds of kilowatts) to transfer through a large air-gap (10-40 cm) by magnetic induction. Consequently, strong electromagnetic near fields are produced around the WPT system during operation. These fields may exceed the reference and/or the basic restrictions (maximum allowable) levels defined by the international standards and guidelines [4]–[6]. These fields may have the possibility of inducing high field strength in the body tissue of humans and living organisms existing in the proximity of the WPT system. This raises the important safety issues of the whole-body heat stress, excessive localized tissue heating, and adverse health effects [7], [8]. Moreover, these EMFs may have the possibility of causing malfunction for the implantable medical devices (IMDs) operating near the system [9]. Therefore, precautions need to be considered during the design and manufacturing stages to ensure the electromagnetic compatibility (EMC) with the international standards. In addition, after manufacturing and installing the WPT system in the vehicle, tests for EMF are mandatory to ensure the EMC before market release. Several studies can be found in the literature that provide assessment and evaluation analysis for EMFs of WPT system in EVs applications [9]–[15]. These studies deal with the EMFs exposure during the design stage. Moreover, all these works are based on numerical simulation for the WPT coupler and human body to test the basic restriction limits. Few publications that mix between simulation and experimental evaluation for the EMFs from WPT system in EVs applications can be found in the literature [16], [17]. However, in these studies test prototypes were utilized with low power transfer capability that does not match with the EV requirements. Also, the EV's body shielding effect was simply considered using a metal plate, which does not reflect the actual behavior of the whole vehicle body on the EMF measurements.

This work was authored in part by the National Renewable Energy Laboratory, operated by Alliance for Sustainable Energy, LLC, for the U.S. Department of Energy (DOE) under Contract No. DE-AC36-08GO28308. Funding provided U.S. Department of Energy Office of Energy Efficiency and Renewable Energy Vehicle Technologies Office. The views expressed in the article do not necessarily represent the views of the DOE or the U.S. Government. The U.S. Government retains and the publisher, by accepting the article for publication, acknowledges that the U.S. Government retains a nonexclusive, paid-up, irrevocable, worldwide license to publish or reproduce the published form of this work, or allow others to do so, for U.S. Government purposes.

Different from the presented studies in the literature, this paper presents an assessment methodology for the electric and magnetic fields from an in-vehicle WPT system. The proposed methodology is based on near-field measurements to evaluate the reference levels of the EMFs. A 25 kW WPT system installed in a NREL shuttle is utilized for conducting the tests. The work provides technical considerations for the test set-up, device and points. In addition, a practice to consider the misalignments between the two pads during the tests is presented.

II. DESCRIPTION OF THE IN-VEHICLE WPT SYSTEM UNDER TEST

The EMF tests are accomplished for a commercial 25-kW WPT system from Momentum Dynamics that was installed in a NREL electric shuttle. The description of the system under consideration is discussed in this section.

A. WPT System Description

A block diagram for the WPT system under test is indicated in Fig. 1. The system consists of two electrically isolated assemblies: ground (GA) and vehicle (VA). The GA contains the primary transmitter pad, which is connected to a three-phase supply through a primary power module (PPM). The VA comprises of a secondary receiver pad, which is coupled to the EV's battery via a secondary electronics module (SEM). The power is moving from the GA to VA by magnetic induction with the two sides operating at resonance. The PPM consists of a three-phase rectifier, dc-link capacitor, high-frequency inverter and primary compensation network. The SEM comprises of a secondary compensation network, single-phase rectifier and filter. Symmetrical coupler with rectangular structure (two identical power pads) design is considered in the system. The assemblies are communicating with each other through wireless data link. The system is capable of transferring 25-kW through a 9.5-inch air-gap. The system is intended for heavy-duty automotive application (which is in the range of 22 to 200 kW) and is designed to operate at 20 kHz resonant frequency, which is one of the frequency bands proposed in IEC 61980 standard [5].

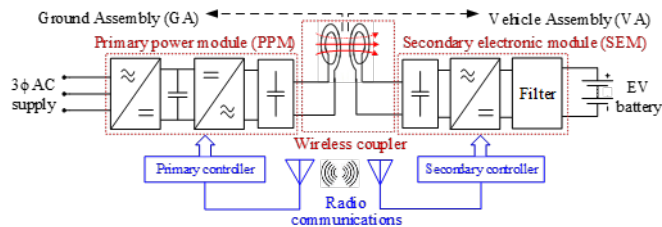


Fig. 1: Block diagram of WPT system under test.

B. Description of Wirelessly Charged NREL Shuttle

The WPT system is installed in one of the shuttles operating inside NREL campus for employee transportation. The shuttle is pure electric with 62.1 kWh battery capacity and 100 miles range. The shuttle has a curb weight of 7600 pound including the VA and it fits 16 passengers at full capacity. The GA of the WPT system is implemented at the parking lot at NREL garage

area, while the VA is installed in NREL on-demand shuttle. The shuttle with the WPT system is depicted in Fig. 2. The shuttle is intended to operate between NREL campuses based on the employees' request. It is able to charge wirelessly during the idle time where there is no demand. The installment of the VA of the WPT system underneath the shuttle is described in Fig. 3. This position was chosen because it was the only location available on the shuttle to make the installation. However, the recommended installation position on the vehicle, based on the SAE J2954 standard, is generally right behind the front axle of the vehicle [18].

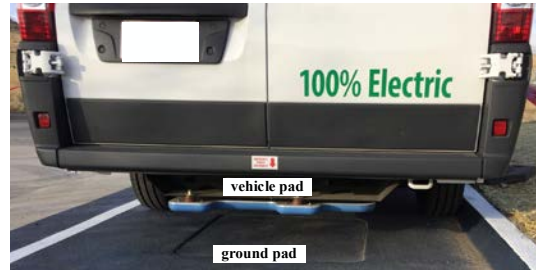


Fig. 2: Wirelessly charges NREL shuttle under test.

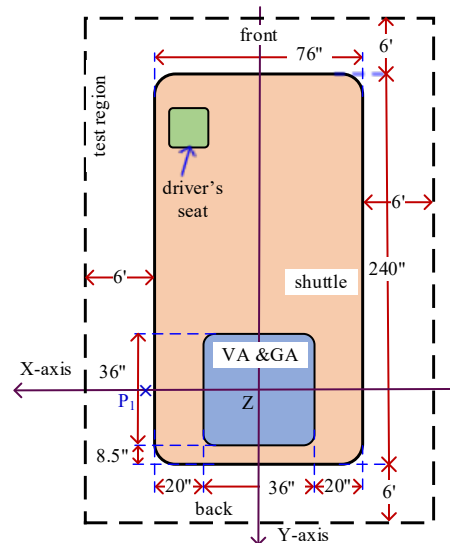


Fig. 3: The position of the VA and GA underneath the shuttle at perfect alignment.

III. NEAR FIELD TEST METHODOLOGY

Measurements for the electric and magnetic fields are accomplished in the area around the WPT system and the shuttle. Details about the measuring device and the test set-up are presented in this section.

A. EMFs' Measuring Device

A low frequency isotropic field probe-analyzer (Model EHP-50D, Narda, Pfullingen, Germany), 5 Hz -100 kHz bandwidth, was utilized. It includes XYZ field simultaneous measurements with a built-in spectrum analyzer. The probe is connected to a PC by a fiber optic cable. A dedicated software manages the probe setting, data acquisition and storage. The chosen probe settings are indicated in Table I.

TABLE I.
SETTINGS OF EHP-50D PROBE

Parameter	Value
Span	3-100 kHz
Measurement mode	Max RMS over 30 sec.
Hold Maximum	Enable
Showing XYZ measurements	Enable
Measuring Range	Small range
Units	B (μ T) & E (V/m)

B. EMFs Test Set-up

To start the EMFs measurements, the area of the WPT system is prepared and organized as follows:

1) Defining the reference coordinates

Two coordinate systems are defined based on the test region. For tests under and around the shuttle, the reference coordinates are chosen to have an origin that matches with the center of the ground pad. This is because the VA position is variable depending on the shuttle position. For tests inside the vehicle, the reference coordinates are chosen to have an origin that matches with the center of the vehicle pad. The two coordinates are identical during the perfect alignment position, as indicated in Fig. 3. The misalignments are defined by measuring the distances in X and Y directions between the centers of the pads. The positive Z-direction starts from the ground floor (the upper surface of the ground pad) and extends perpendicular to the ground plan.

2) Defining a marked safety perimeter

Since the tests are conducted at the actual operating site, a marked safety perimeter needs to be defined around the WPT system and the shuttle under test; and persons should not enter this area when the WPT fields are active. The goal is to guarantee that the area outside the test region is safe for the public during the continued testing. This area is defined by establishing a restricted area with distance > 3 m around the system under test [18], and measuring the EMFs at the perimeter with the system operating at its rated power. If the fields levels exceed the standard limits, the system should be shut-down, and the perimeter will be increased to a wider distance. If the fields are below the standard limits, the perimeter will be reduced until the fields at the perimeter are at the recommended safe limits. However, if the fields around the vehicle meet the standard limits, the perimeter need to be defined to allow enough test area for the workers, which can be estimated with 6-7 feet around the system, as indicated in dash in Fig. 3.

C. Defining the Worst Operating Condition

The stray EMFs from the WPT system are significantly affected by the misalignment between the transmitter and receiver. Perfect alignment conditions result in minimum stray fields around the system and maximum fields between the two pads. However, increasing the misalignments enhances the

leakage fields around the system and reduces the coupled fields between the pad. Thus, for each test region, the worst alignment conditions need to be defined and considered during the tests. This is achieved by applying different combinations of misalignment and taking the field measurements at few points that represent the worst scenarios. By comparing the results of all the cases, the worst operating condition can be defined. In addition to considering the misalignment in X, Y and Z directions, the pitch, roll and yaw misalignment need to be considered as well. However, this may be difficult to be realized with a real vehicle test. Therefore, the possible combinations are considered. However, all combinations are necessary for a prototype tests [18].

IV. TEST ZONES AND STANDARD SAFETY LIMITS

A. EMF Test Zones

Several categories of EMF tests need to be conducted based on the region under test. According to the WPT standards SAE J2954 [18] and IEC 61980 [5], the most concern zone is right between the two coils and around the coils but still under the vehicle, which is named region 1 in J2954 standard. This area contains the strongest EMFs, but it is noted that it is not directly exposed to humans or animals at all time. The EMFs in this region is very strong and typically exceed the reference and the basic restriction limits defined by the standards. Therefore, the EMF exposure in region 1 needs to be prevented either by applying active or passive access control or implementing detection and shutdown before ingress into areas where such exposure could occur [18]. Addressing the EMF exposure in region 1 is out of scope of this publication.

The other important regions of concern that need consideration are near the charger and around the vehicle (not under the car), which is named region 2; and inside the car, which refers to region 3. In addition to these three regions, it is important to test the area around the PPM with which the public is likely to be exposed. The EMFs levels in region 2, 3 and around the PPM should comply with the standard limits presented in Table II and discussed in-details in the next section.

B. EMFs Standard Limits

A variety of standards and guidelines have been developed to limit potentially adverse effects due to EMF exposure, such as 1998 and 2010 ICNIRP guidelines, IEEE C.95.1, IEC 61980-3 and ACGIH TLV 2017. These standards have defined the EMF limits based on two levels: *Basic Restrictions (Maximum Allowable Levels)*, and *Reference Levels*. *Basic Restrictions* represent the maximum values of the electric fields and current density that are allowed to be induced inside the human body. Because of the difficulty to measure the fields inside the body, the standards have defined the *reference levels*, which represent the external magnetic and electric fields that result in the induced fields inside the body. The compliance with the reference levels guarantees the compliance with the basic restriction. However, exceeding the reference levels does not mean that the basic restrictions are violated. Additional tests need to be conducted to ensure the compliance with the basic

restrictions. This work is intended for testing the reference levels in region 2, 3 and around the PPM. A comparison for the EMFs reference limits for general public and occupational exposure for the commonly used standards in industry for WPT system, is presented in Table II.

TABLE II.
STANDARDS EMF REFERENCE LIMITS FOR GENERAL PUBLIC AND OCCUPATIONAL EXPOSURE

standard	Magnetic field, B_{rms} (μT)		Electric field, E_{rms} (V/m)	
	general public	occupational	general public	occupational
ICNIRP 2010	27	100	83	170
IEEE C.95.1-2014 (3 kHz -5 MHz)	205	615	614	1842
ACGIH TLV 2017 (2.5-30) kHz	---	200	---	1842

V. RESULTS AND DISCUSSION

The 25-kW WPT system installed in NREL shuttle and is operated at rated power with a 20 kHz resonant frequency. The operating frequency changes from 19 to 21 kHz based on the alignment position. EMF tests in region 2, 3 and around the PPM are conducted and compared with the standard levels. The tests are achieved using EHP-50D probe-analyzer with the settings defined in Table I. In addition, numerical simulations for the wireless coupler were carried out with the finite element analysis software JMAG. The model includes material properties like magnetic permeability and electrical conductivity. A circuit model provides a source of current density for the coils. Eddy currents induced in nearby conductors are modeled and contribute to the total calculated magnetic fields. The vehicle shielding effect is emulated in the model using a large aluminum plate above the vehicle's pad with same dimensions as the bus (240"x76"x0.5"). Geometries are significantly simplified but correspond closely to the physical device. The finite element mesh maximum dimension varies from 10 mm to 100 mm. The experimental and simulated results are presented and discussed in this section.

A. Region 2 Test Results

The EMFs are measured at different points around the bus to mimic a person touching the bus's body. As an example, the measured FFT distribution of the magnetic and electric fields at point P_1 in Fig. 2 are presented in Figs. 4 and 5. These measurements are taken at height of 6.25" from the ground, which represents the worst situation, where the sensor is aligned between the two pads. As it can be seen, the highest fields' peak appeared at the fundamental frequency (21 kHz). Smaller peaks appeared at the higher harmonic frequencies. The odd harmonics are larger in both magnetic (B) and electric (E) fields, due to the HF square wave voltage from the HF inverter. Moreover, it can be noted that the maximum values of both fields are less than the standard reference limits including ICNIRP 2010, which has the most restricted limits.

The EMFs in region 2 are very sensitive to the misalignment conditions. Therefore, five different

misalignment conditions are established and tested to define the worst operating scenario. In all positions, the system was operating at full power and the probe height is 6.25". The tested positions are depicted in Fig. 6. The measured maximum RMS values for the electric and magnetic fields at point P_1 in Fig. 2 are presented in Table III. The table shows that the EMFs change with the misalignment, with the worst values appearing when the secondary side is shifted away from the measuring point. However, even with the misalignments, the EMFs are below the standard reference limits.

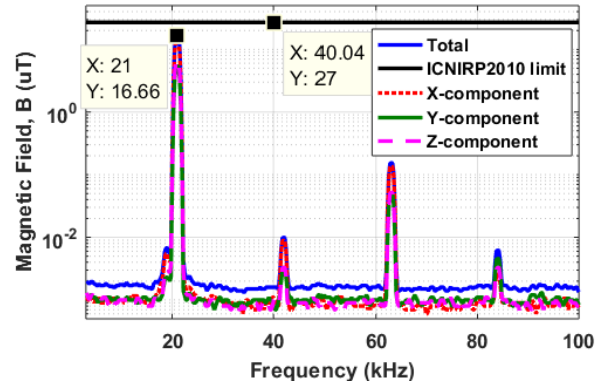


Fig. 4: Measured FFT distribution of magnetic fields at region 2 (point P_1) with full power transfer (Height = 6.25").

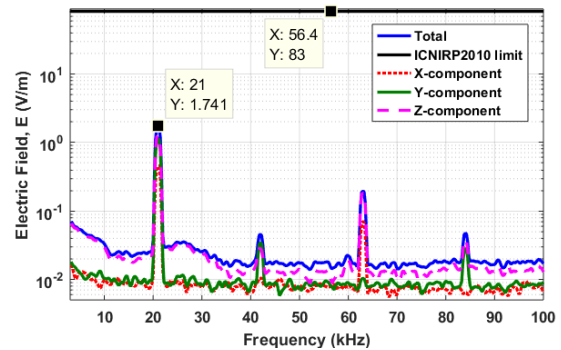


Fig. 5: Measured FFT distribution of electric fields at region 2 (point P_1) with full power transfer (Height = 6.25").

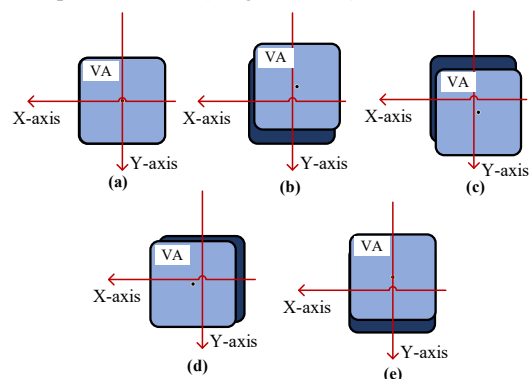


Fig. 6: Different misalignment positions to define the worst case.

- (a) Position I ($\Delta X=0$, $\Delta Y=0$ and $Z=9.5''$).
- (b) Position II ($\Delta X=-1''$, $\Delta Y=-2.5''$ and $Z=9.5''$).
- (c) Position III ($\Delta X=-1''$, $\Delta Y=2.25''$ and $Z=9.5''$).
- (d) Position IV ($\Delta X=1.5''$, $\Delta Y=-1''$ and $Z=9.5''$).
- (e) Position V ($\Delta X=0$, $\Delta Y=-2.25''$ and $Z=9.5''$).

TABLE III.
MEASURED EMFS AT POINT P1 REGION 2 AT DIFFERENT
MISALIGNMENT AT 21 KHZ

Misalignment	Max B_{rms} (μT)	Max E_{rms} (V/m)
Position I	16.661	1.7414
Position II	18.380	2.4091
Position III	17.696	2.5345
Position IV	17.152	1.7147
Position V	18.526	2.0853

B. Test Results around PPM

EMF measurements are taken around the PPM cabinet with the system transferring the full power. The test points are depicted in Fig. 7. The EMFs are measured at two heights LOW (L), which is 6.25" from the ground; and HIGH (H), which is 26.25" from the ground. The test results are presented in Table IV. It can be noted that the EMFs at the H level are larger than those at L level. This is because the higher level is closer to the HF inverter. In general, very low EMFs are experienced around PPM compared with the standard limits.

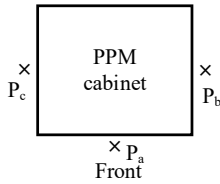


Fig. 7: Test points around the PPM cabinet.

TABLE IV.
MEASURED EMFS AROUND THE PPM AT 21 KHZ

Test Point	Max B_{rms} (μT)	Max E_{rms} (V/m)
$P_{a,L}$	0.7251	0.1617
$P_{b,L}$	0.3293	0.1469
$P_{c,L}$	0.2375	0.1416
$P_{a,H}$	1.1235	0.1839
$P_{b,H}$	0.5735	0.1125
$P_{c,H}$	0.3472	0.1106

C. Region 3 Test Results

A third test is conducted for region 3, which covers the area inside the bus. The measurements inside the bus are taken while the system is at misalignment of ($\Delta X=0$, $\Delta Y=2.25$ " and $Z=9.5$ "), which represents the worst case for region 3 since the bus floor will be exposed to the largest amount of stray field. Since the driver will be inside the bus during the charging, the EMFs at the driver's seat are necessary to be measured and compared with the exposure limits. Therefore, the EMFs at driver's seat are recorded at the three points indicated in Fig. 8. Point A is at height of 6.25" from the floor of the bus, Point B is at height of 6.25" from the seat, and Point C is at height of 26.25" from the seat. The test results are indicated in Table V. As it can be seen, the EMFs are negligible at the driver position, due to the shielding effect from the bus body and the large distance between the WPT system and the seat.



Fig. 8: Test points for the driver's seat inside the bus.

TABLE V.
MEASURED EMFS AT THE DRIVER'S SEAT

Test Point	Max B_{rms} (μT)	Max E_{rms} (V/m)
P_A	0.0328	0.0633
P_B	0.0068	0.0380
P_C	1.0362	0.0257

The other region of interest inside the bus to be tested, is the area right above the vehicle assembly. To test this area, new coordinates ($X'Y'Z'$) are defined inside the bus with an origin that matches with the center of the vehicle pad, as described in Fig. 9. The Z' axis starts from the floor of the bus and extends perpendicular to the floor plan. The magnetic fields are measured along X' and Y' axes at the points indicated in Fig. 9.

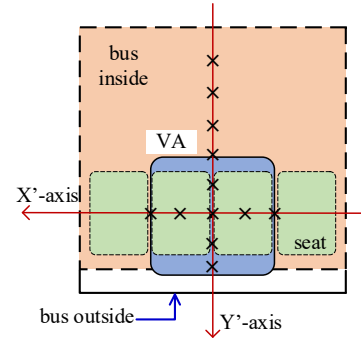


Fig. 9: Test points over the vehicle pad inside the bus.

The test results are compared with the numerical analysis data and presented in Figs. 10 and 11. As can be seen in Fig. 10, the magnetic field in X' direction shows a peak value at the center of the pad and decreases gradually around the center, which matches with the rectangular structure of the wireless pad. Symmetrical field distribution is experienced in X' direction due to the zero misalignment in X' axis ($\Delta X=0$). On the other hand, the magnetic field along Y' axis (Fig. 11) shows a large value at the center and decreases gradually in -ve Y' direction. However, it keeps increasing in +ve Y' direction. This behavior is due to two reasons: 1) the misalignment in Y direction ($\Delta Y=2.25$ "), 2) the installation position of the vehicle pad, which is at the back of the bus. This makes the back of the bus exposed to higher leakage flux and less shielding from the

bus body. Although the trends for both the measured and simulated results are similar, there is significant differences among the values. This is due to the simplifications in the finite-element model which does not reflect the actual impact of the vehicle body and components. In addition, extra shields exist in the actual vehicle that are not considered in the model. In Fig. 10 the experimental results show faster drop in the fields around the center than the simulated data. This is because of the measurements are conducted above the back seats, which provide extra shielding effects. Overall, all the magnetic field measurements inside the bus are very low compared to the standard limits.

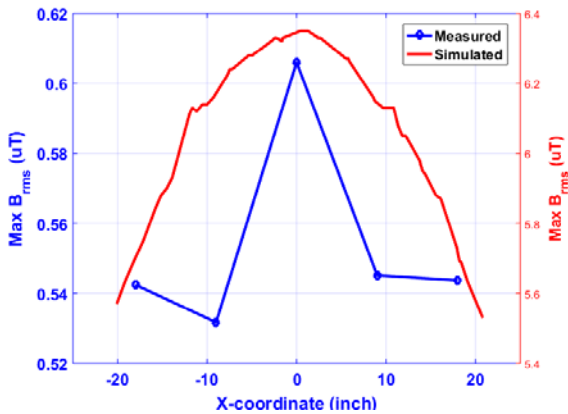


Fig. 10: Magnetic field along X'-axis over the vehicle pad inside the bus at a height of 27.25" from the floor of the bus.

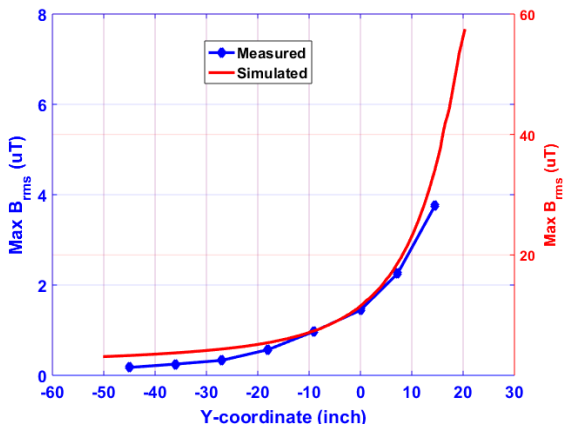


Fig. 11: Magnetic field along Y'-axis over the vehicle pad inside the bus a height of 6.25" from the floor of the bus.

VI. CONCLUSION

The paper presents a near-field analysis for the electromagnetic fields due to 25 kW wireless power transfer system for heavy duty electric vehicles. The tests are conducted with the WPT system physically installed in a NREL electric shuttle. A detailed description for the EMF tests around the WPT system is presented. Test results around the bus (region 2), inside the bus (region 3) and around the primary power module cabinet are presented and discussed in comparison with the reference levels defined by the international standards and guidelines.

Overall, the experimental results show that the WPT system under test meets the requirements for the human exposure to the EMFs from the WPT system.

REFERENCES

- [1] A. A. S. Mohamed and O. Mohammed, "Physics-Based Co-simulation Platform with Analytical and Experimental Verification for Bidirectional IPT System in EV Applications," *IEEE Trans. Veh. Technol.*, vol. P.P, no. P.P, 2017.
- [2] A. Daga, J. M. Miller, B. R. Long, R. Kacergis, P. Schrafel, and J. Wolgemuth, "Electric Fuel Pumps for Wireless Power Transfer: Enabling rapid growth in the electric vehicle market," *IEEE Power Electron. Mag.*, vol. 4, no. 2, pp. 24–35, Jun. 2017.
- [3] A. A. S. Mohamed, C. R. Lashway, and O. Mohammed, "Modeling and Feasibility Analysis of Quasi-Dynamic WPT System for EV Applications," *IEEE Trans. Transp. Electrification*, vol. 3, no. 2, pp. 343–353, Jun. 2017.
- [4] "IEEE Standard for Military Workplaces—Force Health Protection Regarding Personnel Exposure to Electric, Magnetic, and Electromagnetic Fields, 0 Hz to 300 GHz," *IEEE Std C951-2345-2014*, pp. 1–69, May 2014.
- [5] "IEC 61980-1:2015/COR1:2017 | IEC Webstore." [Online]. Available: <https://webstore.iec.ch/publication/59640>. [Accessed: 11-Apr-2018].
- [6] International Commission on Non-Ionizing Radiation Protection, "Guidelines for limiting exposure to time-varying electric and magnetic fields (1 Hz to 100 kHz)," *Health Phys.*, vol. 99, no. 6, pp. 818–836, Dec. 2010.
- [7] W. Zhang, J. C. White, A. M. Abraham, and C. C. Mi, "Loosely Coupled Transformer Structure and Interoperability Study for EV Wireless Charging Systems," *IEEE Trans. Power Electron.*, vol. 30, no. 11, pp. 6356–6367, Nov. 2015.
- [8] H. Jiang, P. Brazis, M. Tabaddor, and J. Bablo, "Safety considerations of wireless charger for electric vehicles #x2014; A review paper," in *2012 IEEE Symposium on Product Compliance Engineering (ISPC)*, 2012, pp. 1–6.
- [9] T. Hikage, M. Yamagishi, K. Shindo, and T. Nojima, "Active implantable medical device EMI estimation for EV-charging WPT system based on 3D full-wave analysis," in *2017 Asia-Pacific International Symposium on Electromagnetic Compatibility (APEMC)*, 2017, pp. 87–89.
- [10] A. Christ, M. Douglas, J. Nadakuduti, and N. Kuster, "Assessing Human Exposure to Electromagnetic Fields From Wireless Power Transmission Systems," *Proc. IEEE*, vol. 101, no. 6, pp. 1482–1493, Jun. 2013.
- [11] S. Park, "Evaluation of Electromagnetic Exposure During 85 kHz Wireless Power Transfer for Electric Vehicles," *IEEE Trans. Magn.*, vol. 54, no. 1, pp. 1–8, Jan. 2018.
- [12] T. Shimamoto, I. Laakso, and A. Hirata, "Internal electric field in pregnant-woman model for wireless power transfer systems in electric vehicles," *Electron. Lett.*, vol. 51, no. 25, pp. 2136–2137, 2015.
- [13] A. A. S. Mohamed, A. Berzoy, and O. A. Mohammed, "Physics-based FE model and analytical verification of bi-directional inductive wireless power transfer system," in *2016 IEEE/ACES International Conference on Wireless Information Technology and Systems (ICWITS) and Applied Computational Electromagnetics (ACES)*, 2016, pp. 1–2.
- [14] E. Yavolovskaya *et al.*, "Simulation of human exposure to electromagnetic fields of inductive wireless power transfer systems in the frequency range from 1 Hz to 30 MHz," in *2016 International Symposium on Electromagnetic Compatibility - EMC EUROPE*, 2016, pp. 491–496.
- [15] E. Yavolovskaya *et al.*, "Low frequency human exposure analysis for automotive applications," in *2017 International Symposium on Electromagnetic Compatibility - EMC EUROPE*, 2017, pp. 1–6.
- [16] J. Chakarothai, K. Wake, T. Arima, S. Watanabe, and T. Uno, "Exposure Evaluation of an Actual Wireless Power Transfer System for an Electric Vehicle With Near-Field Measurement," *IEEE Trans. Microw. Theory Tech.*, vol. 66, no. 3, pp. 1543–1552, Mar. 2018.
- [17] R. Pinto *et al.*, "Exposure assessment of stray electromagnetic fields generated by a wireless power transfer system," in *2015 9th European Conference on Antennas and Propagation (EuCAP)*, 2015, pp. 1–4.
- [18] "J2954A (WIP) Wireless Power Transfer for Light-Duty Plug-In/ Electric Vehicles and Alignment Methodology - SAE International." [Online]. Available: <http://standards.sae.org/wip/j2954/>. [Accessed: 10-Jul-2016].